

CO₂-Enhanced Transport of Small Molecules in Thin PMMA FilmsTi Cao,[†] Keith P. Johnston,^{*,‡} and S. E. Webber^{*,†}*Departments of Chemistry and Biochemistry and Chemical Engineering, The University of Texas at Austin, Austin, Texas 78712**Received October 4, 2004; Revised Manuscript Received December 8, 2004*

ABSTRACT: Steady-state fluorescence measurements have been used to measure the rate of transport of a fluorescent probe (pyrene) out of ca. 200–340 nm thick films of poly(methyl methacrylate) (PMMA) in contact with supercritical CO₂ at pressures in the range 34–76 bar (estimated CO₂ content in the film from 0.06 to 0.17 weight fraction) and several temperatures (35, 50, and 65 °C). At constant temperature, the estimated pyrene diffusion coefficient increases by approximately 4 orders of magnitude from the lowest to the highest CO₂ content (e.g., from ca. 5×10^{-15} cm²/s for ca. 0.08 CO₂ weight fraction to ca. 10^{-10} cm²/s for ca. 0.17 CO₂ weight fraction at 35 °C). We compare the present results to our earlier study of CO₂-swollen polystyrene (PS) and find: (1) For similar pressures of CO₂ at the same temperature, the enhancement of the pyrene diffusion coefficient is larger in PMMA than in PS, presumably as a consequence of the higher solubility of CO₂ in PMMA; and (2) at similar CO₂ contents, the pyrene diffusion coefficient is higher in PS than in PMMA by several orders of magnitude, which we attribute to the PS higher free volume for pyrene diffusion compared to PMMA for CO₂-swollen films.

Introduction

It is well known that CO₂ may act as a polymer processing aid. It has been demonstrated that the glass transition temperature of many polymers can be significantly lowered by exposure to CO₂, as with any swelling solvent.¹ Similarly, the rate of transport of small molecules into and out of polymers has been demonstrated to increase in the presence of CO₂. However, quantification of these effects has occurred only recently, starting with the 1992 paper of Berens et al.²

The use of fluorescence techniques to study the movement of either small molecules or tagged polymers in polymer solids has been well established by the groups of M. A. Winnik³ and J. M. Torkelson,⁴ and these techniques have recently been applied by Gupta et al. to the study of small-molecule probe diffusion in CO₂ swollen polystyrene.⁵ The present paper is a continuation of our earlier fluorescence study of CO₂-swollen polystyrene (PS) films,⁶ applied to PMMA films.

The method we use here is simple to carry out, as we simply observe the loss of fluorescence of a small molecular probe (pyrene) by virtue of its transport out of the film into the CO₂ phase in contact with it. Of course, for our method to work, it is essential that the probe have sufficient CO₂ solubility that transport out of the film is facile.⁷ While many typical fluorescent probes have very low solubility in CO₂, this transport process can still be highly efficient because of their very high diffusion constant in CO₂. The sensitivity advantage of fluorescence techniques can be very important in measurements of diffusion processes. Since the time required for molecular transport out of an object scales as l^2/D (D is the diffusion coefficient of the molecule, l is the dimension of the object), for small diffusion constants, it is essential that l be small in order to keep the experimental time manageable.⁸ In the present case, we use films of ca. 200–340 nm thickness and present

measurements of the probe diffusion coefficient as low as ca. 10^{-14} cm²/s. We would have no difficulty measuring transport processes on films substantially thinner than this, but it is expected as the film thickness approaches the radius of gyration of the polymer that “confinement effects” would be observed.⁹

Experimental Section

The methods used herein are essentially identical to our earlier paper,⁶ and we describe our methodology in the following.

Purification and Characterization of Pyrene and PMMA. Pyrene was obtained from Eastman Kodak and purified by recrystallization from ethanol three times. The purified pyrene quality was checked by UV-absorption and fluorescence spectra.

PMMA from Scientific Polymer Products, Inc. (nominal M_w = 75 000, lot# 25 cat#037B) was purified by reprecipitation twice from HPLC grade methylene chloride using HPLC-grade methanol as the precipitant and once from HPLC-grade benzene using HPLC-grade heptane as precipitant. The last precipitate was dissolved in benzene and vacuum freeze-dried followed by vacuum-drying at 85°C for 15 h to remove all solvent in the sample. The characterization of the purified sample by GPC was carried out using a system employing with four μ -Styragel columns, pore size ranging from 500 to 10^5 Å, connected in series and equipped with a Water R401 differential refractometer, a Perkin-Elmer LS fluorescence detector and a HP 1050 UV–visible diode array connected in series. Degassed HPLC-grade THF (from Fisher) was used as the mobile phase at 1.5 mL/min and four narrow-distribution PMMA standards from Scientific Polymer Products, Inc. were used for molecular-weight and its distribution analysis. No fluorescence impurities or monomeric and oligomeric methyl methacrylate were found in the purified sample. Its weight average molecule weight and molecular weight polydispersity (M_w/M_n) were 1.26×10^5 and 2.40 respectively (compared to 7.76×10^4 and 6.76 for unpurified sample). The glass transition of the purified PMMA was measured on a Perkin-Elmer DSC-7. The temperature at the inflection point in the endotherm curve extrapolated to zero heating rate was considered to be the DSC glass transition temperature of PMMA (110.9 °C).

Preparation of Polymer Films. Purified pyrene (15 mg) was dissolved in 10 mL of HPLC-grade toluene. Then 156 mg

* Authors to whom correspondence should be addressed.

[†] Department of Chemistry and Biochemistry.

[‡] Department of Chemical Engineering.

of purified PMMA was mixed with 2.33 mL of HPLC-grade toluene and 0.67 mL of the pyrene-toluene solution. The mixture was heated to 60 °C and mixed briefly on a Vortex-Genie mixer to ensure a homogeneous solution. The solution was maintained at 60 °C overnight and then passed through a 0.45 μm pore size PTEF filter twice. The PMMA-pyrene film was directly spin-coated from the filtered solution onto a clean polished sapphire window used for the high-pressure fluorescence cell⁶ at 2000 or 5000 rpm using Photo-Resist Spinner model 1-EC101D-R435 (Headway Research, Inc.). To relieve any strain in the film, the film on window was annealed in argon and pyrene vapor at 115 °C for ca. 1 h. The pyrene loss in the film during annealing was checked by fluorescence emission to be 20 wt%. With the use of the above protocol, reproducible films of thickness ca. 200–340 nm could be reliably produced. Because of the presence of excess pyrene during this step, it is assumed that the distribution of pyrene in the film is uniform.

The film thickness was measured using an ALPHA-STEP 200 profilometer (Tencor Instruments) with software version 3.7-2 before and after fluorescence experiments. The thickness was taken as the average over at least six points on the film, with a standard deviation of 5 nm). The surface quality of the films and adhesion to the substrate was very good both before and after the fluorescence experiment, as judged by the naked eye and from the profilometer measurements. The film thickness did not change after exposure to CO₂ within experimental error. Of course, the film swells during CO₂ exposure, as will be discussed later.

Fluorescence Experiments. All fluorescence signals were collected using front face geometry as the ratio of the signal to the reference signal (*S/R* mode). The width of the excitation and emission monochromator slits was 2 mm (equivalent to 3.4 nm bandwidth) for both emission and excitation spectra. The excitation wavelength of emission spectrum was 340 nm. For all time base scans, the excitation was at 340 nm with a 3.4 nm bandwidth and the emission was collected at 396 nm with 10.2 or 13.6 nm bandwidth. We did not observe any shift in the excitation or emission spectrum of pyrene after the introduction of CO₂. Although the fluorescence intensity can be measured immediately after the introduction of the CO₂, the first few points are not expected to be typical of the CO₂-swollen and equilibrated film and we typically exclude the initial data from the data analysis (see later discussion).

Loss of Pyrene into Vacuum. We also studied the pyrene release from PMMA film into vacuum for a range of temperatures near the glass transition. We found that the application of a modest vacuum (floor pump with an ultimate vacuum of ca. 30 milliTorrs plus a liquid nitrogen cold trap) resulted in steady loss of pyrene fluorescence that could be successfully interpreted using standard diffusion equations (see next section). After the temperature of the sample compartment and the sapphire window plus film was judged to be equilibrated, the vacuum was switched on. From the point of view of the data analysis, so long as a relatively small fraction of pyrene has escaped from the film during the temperature equilibration, the choice of the time point to designate as $t = 0$ is not critical to the analysis. In principle the rate of loss of pyrene into the vacuum depends not only on the diffusivity of the pyrene but also the vapor pressure of the pyrene at a given temperature (the same would be true for the loss to supercritical CO₂). Both the early time and late time release can be fit to the diffusion equation, yielding essentially the same diffusion constants, as is the case for the release of pyrene into supercritical CO₂ (see later).

Data Analysis. Diffusion out of a plane sheet (infinite film) into an infinite reservoir (e.g., the concentration of the probe outside the slab is close to zero at all time) with a time-independent diffusion constant, D , yields the following early-

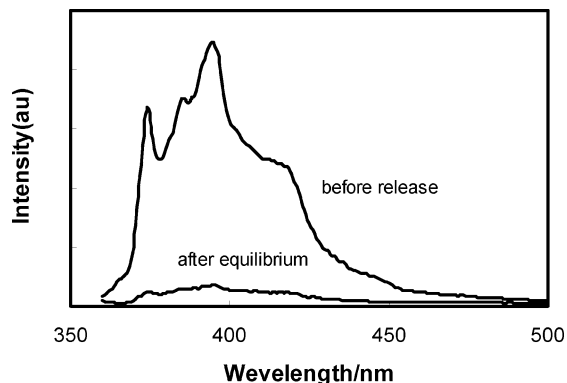


Figure 1. Emission spectra of pyrene in PMMA dry film ($\delta = 214$ nm) before pyrene release and after equilibration in CO₂ at 60.5 bar and 65 °C.

and late-stage solutions for the fraction of probe that has been lost from the film:¹⁰

When $M_t/M_\infty < 0.6$:

$$\frac{M_t}{M_\infty} \approx 2 \left(\frac{Dt}{\pi l^2} \right)^{1/2} = k_1 t^{1/2} \quad (1)$$

When $M_t/M_\infty > 0.6$:

$$\ln \left(1 - \frac{M_t}{M_\infty} \right) \approx \ln(8/\pi^2) - \frac{\pi^2 Dt}{4l^2} = A + k_2 t \quad (2)$$

If we plot M_t/M_∞ versus $t^{1/2}$ at early stage and plot $\ln(1 - M_t/M_\infty)$ versus t at late stage we can obtain D_1 and D_2 from the slopes k_1 and k_2 , respectively. In the present experiments, these two values are found to be in good agreement with each other, consistent with the use of diffusion equations for the data analysis. At very low optical density (such as we have in our very thin polymer films) and in the absence of self-quenching (as evidenced by the absence of the pyrene excimer fluorescence), the total fluorescence is proportional to the amount of fluorophore and we may write

$$\frac{M_t}{M_\infty} = \frac{I_0 - I_t}{I_0 - I_\infty} = F(t) \quad (3)$$

I_0 and I_∞ are the initial and limiting fluorescence intensities from film, respectively.

The volume expansion fraction ($\Delta V/V_0$) and weight fraction of CO₂ in the swollen polymer (w_{CO_2}) are important for correcting and comparing the probe diffusivity for different polymers. The w_{CO_2} and $\Delta V/V_0$ of PMMA under our experimental pressures and temperatures were extrapolated or interpolated from the data presented by Wissinger and Paulaitis,¹¹ Zang et al.,¹² and Hilic et al.¹³

Results

Fluorescence Spectra. The emission spectrum of pyrene from a doped PMMA 214 nm thick film at 65 °C is shown in Figure 1. No excimer fluorescence was observed, which implies that the pyrene is dispersed in the PMMA matrix at the molecular level. The rate of the normalized fluorescence intensity (I_t/I_0) monitored at 396 nm depends strongly on the CO₂ pressure (see Figure 2). According to diffusion theory, the function $F(t)$ should be linear in $t^{1/2}$ for $0 \leq F(t) \leq 0.6$. However, at the beginning (see Figure 2b), there is a clear nonlinearity which must be attributed to the time required for the film to absorb CO₂ and reach equilibrium. Consequently, we use eq 1 for $0.2 \leq F(t) \leq 0.6$. For the late-stage analysis, we use eq 2 for $0.6 \leq F(t) \leq 0.95$.

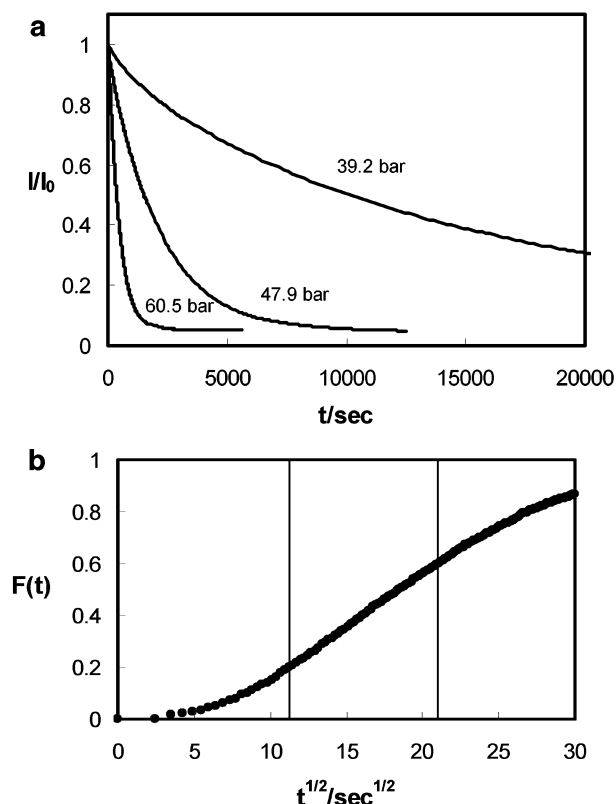


Figure 2. (a) Time-dependent normalized emission intensity of pyrene in PMMA films (ca. 210 nm thickness) exposed to CO₂ at 39.2, 47.9, and 60.5 bar and 65 °C. (b) Plot of $F(t)$ vs $t^{1/2}$ for a PMMA 214 nm thick film exposed to CO₂ at 60.5 bar and 65 °C. The middle section indicated is the range of values that use eq 1 (early stage) for the evaluation of D_1 .

Estimation of Diffusion Constants (Pyrene Extraction into CO₂). Immediately upon introduction of the CO₂, the pyrene fluorescence signal drops because of the change of the refractive index on the inside of the cell so I_0 in eq 3 is obtained from the intensity extrapolated quadratically to time zero using the first four to six points after the introduction of CO₂. I_∞ was estimated from the average intensity over at least 20 points after the fluorescence intensity became constant. Examples of the plots that are used to fit eqs 1 and 2 are given in Figure 3. The values of the diffusion constant using eqs 1 and 2 are denoted D_1 and D_2 , respectively (the experimental values are presented in the Supporting Information for this paper). In the analysis, we use the corrected thickness of the swollen film. It is reasonable to assume that all swelling occurs in the dimension perpendicular to the sapphire window because the film is held firmly in place by the sealing gasket. Therefore, we assume that $l = fl_0$, where l_0 is the dry film thickness and f is the swelling coefficient, $f = V(\text{CO}_2)/V_0 = 1 + \Delta V(\text{CO}_2)/V_0$.

We estimated the weight fraction of CO₂ in swollen PMMA using the data of Wissinger et al.¹¹ and the CO₂ fugacity using the equation of state for CO₂.¹⁴ The values of $\log D_1$ and $\log D_2$ are in close agreement (the $\log D_2$ values are about 0.1 lower than $\log D_1$ at the same pressure, see the Supporting Information), and for all later discussions, we use a simple average of these two values, $\langle \log D \rangle$. We plot $\langle \log D \rangle$ versus P_{CO_2} and f_{CO_2} (fugacity of CO₂) at 35, 50, and 65 °C for PMMA films in Figure 4, and note that at a given P_{CO_2} or f_{CO_2} the diffusion constant at 35 °C is larger than at 50 or

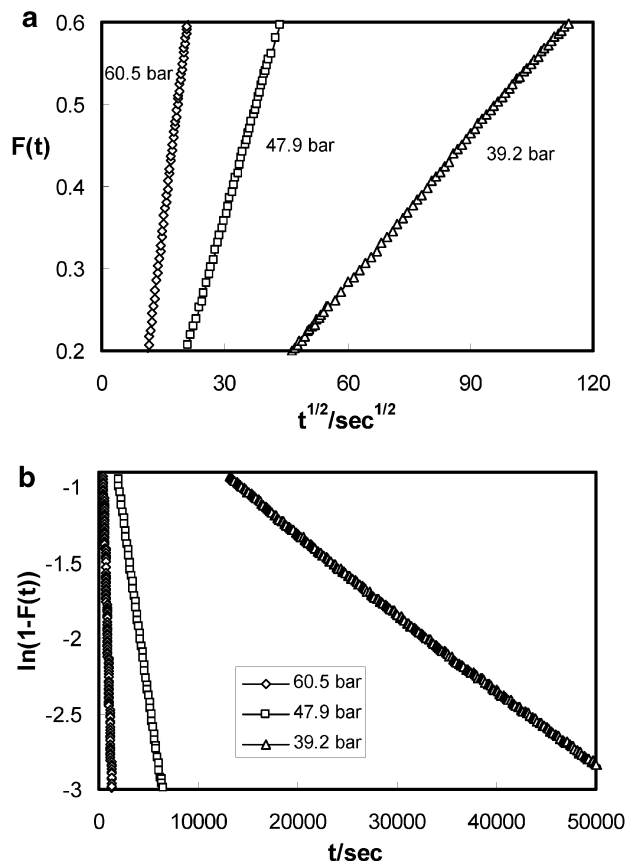


Figure 3. Plot of $F(t)$ vs $t^{1/2}$ (early stage) (a) and $\ln[1 - F(t)]$ vs t (late stage) (b) for PMMA ca. 210 nm thick films exposed to CO₂ at 39.2, 47.9, and 60.5 bar and 65 °C.

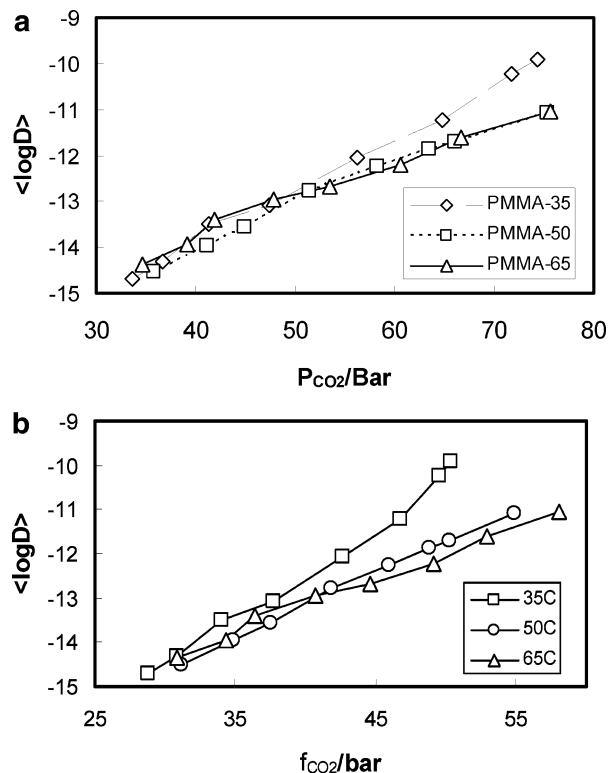


Figure 4. $\langle \log D \rangle$ vs P_{CO_2} (a) and f_{CO_2} (b) at 35, 50, and 65 °C for PMMA films.

65 °C. This is a consequence of the higher solubility of CO₂ in PMMA at the lower temperature. While we do not plot our older data for PS in Figure 4, we note that

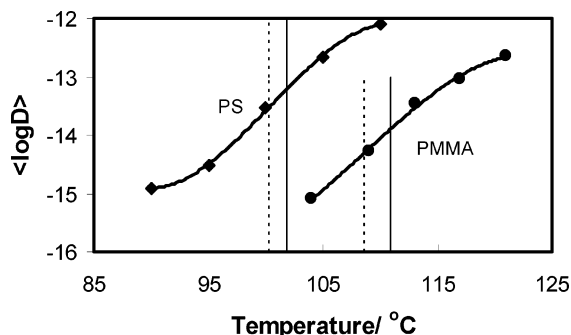


Figure 5. $\langle \log D \rangle$ vs T for the release of pyrene into a vacuum from PS and PMMA films. The vertical lines correspond to T_g derived from the inflection point method (dashed line) and DSC measurement (solid line).

Table 1. $D(T_g, 0)$ Values Estimated from Pyrene Vacuum Release Experiment

polymer	PMMA		PS	
method	$\langle \log D \rangle$	$T_g(^{\circ}\text{C})$	$\langle \log D \rangle$	$T_g(^{\circ}\text{C})$
inflection ^a	-14.28	108.6	-13.49	100.4
DSC ^b	-13.87	110.9	-13.21	101.8

^a The value at the inflection point on the $\langle \log D \rangle$ vs T plot (see text and Figure 5) ^b The value interpolated from the curve of $\langle \log D \rangle$ vs T at the T_g determined by DSC

at any corresponding temperature or P_{CO_2} $\langle \log D \rangle_{\text{PS}}$ is less than $\langle \log D \rangle_{\text{PMMA}}$ (see later discussion).

Estimation of Diffusion Constants for Unswollen Films at T_g (Pyrene Vaporization). The sublimation of pyrene from a polymer film into vacuum is a physical process that is analogous to extraction by CO_2 , and the loss of pyrene fluorescence can be treated using the same equations as discussed above to obtain D_1 and D_2 . These are plotted for PS (using our data from ref 6) and PMMA as a function of T in Figure 5, and as can be seen, the rate of change of these quantities is relatively large in the region of T_g . We empirically estimated our $\log D(T_g, 0)$ values as follows (0 denotes the absence of CO_2): The $\langle \log D \rangle$ vs T plot was fit to a cubic equation, and the inflection point was found by setting the second derivative equal to zero. We also used the DSC T_g of our PS and PMMA samples (see Experimental Section) and determine $\log D(T_g, 0)$ from our cubic fit of the $\langle \log D \rangle$ data. The values of T_g and $D(T_g, 0)$ are collected in Table 1. We note that $(\langle \log D(T_g, 0) \rangle_{\text{PMMA}} - \langle \log D(T_g, 0) \rangle_{\text{PS}}) \approx -0.78$ and -0.66 for the inflection method and DSC method, respectively. Anwand et al. determined the free volume of thin polymeric films using fluorescence probes.¹⁵ The fractional free volumes they measured are 0.0224 and 0.0575 for PMMA and PS, respectively. The higher free volume in PS is presumably responsible for the larger diffusion coefficient of pyrene at T_g compared to PMMA at its T_g (Table 1).

Estimation of P_g Values. In our previous paper,⁶ we attempted to obtain a “ P_g ” value on the basis of the apparent viscosity (or friction factor) of the medium. According to the Stokes–Einstein model, the diffusion coefficient is proportional to the ratio of the temperature and the viscosity at a given temperature (assuming a constant molecular volume). If we propose that in the glassy state the effective viscosity acting on the molecule is a constant (with or without the presence of a swelling solvent), then we can write

$$D(T, P_g) = (T/T_g)D(T_g, 0) \quad (4)$$

where $D(T, P_g)$ denotes the diffusion coefficient of the probe in a swollen film at the CO_2 content that plasticizes it at temperature T and $D(T_g, 0)$ is the diffusion coefficient of the unswollen film at T_g . Note that we compare the 40 °C data for PS with the 35 °C data for PMMA because there were more data points available, which is needed for the inflection point analysis. We take the values of $\log D(T_g, 0)$ in Table 1, as determined by our vacuum experiment, and using eq 4, evaluate P_g (see Table 2). From the value of P_g we can calculate the corresponding value of w_{g, CO_2} . These values are all higher than estimated for PS. The differences between these two polymers is systematic: $P_g^{\text{PS}} > P_g^{\text{PMMA}}$ and $w_g^{\text{PS}} < w_g^{\text{PMMA}}$. We note that it is by no means obvious that a “ P_g ” value determined by a diffusive/transport process will correspond to a “ P_g ” determined by more classic viscoelastic or swelling measurements.

Comparison of PMMA and PS. In the following, we wish to compare our previous results for PS films with the PMMA films. Note that for PS the highest temperature studied was 60 °C, which we will compare with PMMA films at 65 °C (the other temperatures, 35 and 50 °C match exactly). As discussed above, for any P_{CO_2} and temperature combination, $\langle \log D \rangle_{\text{PMMA}}$ is greater than $\langle \log D \rangle_{\text{PS}}$ as a consequence of the higher CO_2 solubility in PMMA. When $\langle \log D \rangle$ values are compared as a function of the weight fraction (w_{CO_2}) of CO_2 in swollen film, a very different picture emerges (see Figure 6). For values of w_{CO_2} that overlap (for 50 °C and 60–65 °C data) there are approximately 4 orders of magnitude difference between D_{PMMA} and D_{PS} , and extrapolating the 35 °C data suggests a similar difference. Presumably this is an effect associated with the relative enhancement of free volume upon CO_2 swelling. The swelling of PMMA and PS has been studied by Wissinger et al.¹¹ and Hilic et al.,¹³ and when we plot their data for $\Delta V/V_0$ (the volume extension fraction due to swelling) vs $\Delta w/w_0$, we see that this parameter is considerably larger for PS (see Figure 7). Presumably, $(\Delta V/V_0)_{\text{PS}} - (\Delta V/V_0)_{\text{PMMA}}$ is a good measure of the CO_2 -induced free volume difference between PS and PMMA. The difference is about 0.02 of the dry polymer volume in the $\Delta W/W_0$ range from 0.07 to 0.09, which is very significant compared to the free volume in glassy PMMA, 0.022.¹⁵ We can estimate the partial molar volume (PMV) of CO_2 in a polymer from the slope of the curve, polymer density, and molecular weight of CO_2 . The PMV of CO_2 in PS and PMMA is 46.1 and 35.4 cm^3/mol , respectively, at 50 °C. Ferguson and von Meerwall¹⁶ have considered the self-diffusion in rubber swollen by two diluents and tested a modification of the Doolittle–Fujita equation for the ratio of the diffusion constant of component, i , in a swollen and an unswollen film:

$$\ln(D(T, v)_i/D(T, 0)_i) = B_{di} \frac{sv}{1 + f_0(T)sv} \quad (5)$$

where $f_0(T)$ is the fractional free volume of the unswollen polymer, v is the volume fraction of the two diluents ($v \equiv v_1 + v_2 \neq 0$), and s is given by

$$s = \frac{\gamma(T) - f_0(T)}{f_0(T)}$$

Table 2. Estimate of P_g for PMMA and PS Using Eq 4

PMMA									
temp	35 °C			50 °C			65 °C		
method	P_g (bar)	w_{g,CO_2}	$\langle \log D \rangle_{P_g}$	P_g (bar)	w_{g,CO_2}	$\langle \log D \rangle_{P_g}$	P_g (bar)	w_{g,CO_2}	$\langle \log D \rangle_{P_g}$
a ^a	36.0	0.0854	-14.37	37.4	0.0718	-14.35	35.5	0.0623	-14.33
b ^b	38.6	0.0934	-13.96	41.3	0.0779	-13.94	39.3	0.0671	-13.92

PS									
temp	40 °C			50 °C			60 °C		
method	P_g (bar)	w_{g,CO_2}	$\langle \log D \rangle_{P_g}$	P_g (bar)	w_{g,CO_2}	$\langle \log D \rangle_{P_g}$	P_g (bar)	w_{g,CO_2}	$\langle \log D \rangle_{P_g}$
a	51.3	0.0532	-13.57	49.9	0.0481	-13.56	45.7	0.0432	-13.55
b	54.2	0.0561	-13.29	52.3	0.0501	-13.27	48.6	0.0456	-13.26

^a Interpolated from the plot of $\langle \log D \rangle$ vs P_{CO_2} at $\log(T/T_g) + \langle \log D \rangle_{T_g(vac)}$ (see text). ^b Like a, except T_g was obtained from DSC measurements.

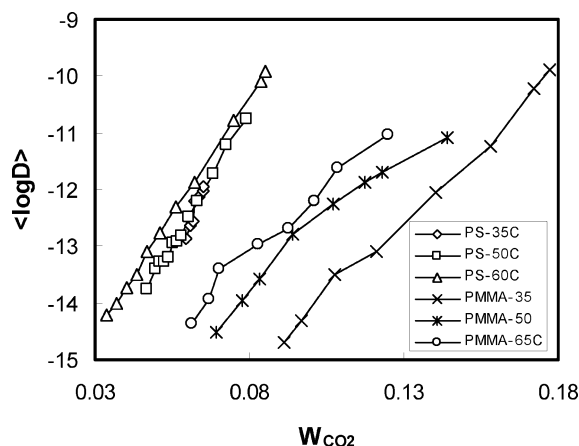


Figure 6. Comparison of $\langle \log D \rangle$ for PMMA and PS films as a function of w_{CO_2} at the temperatures indicated.

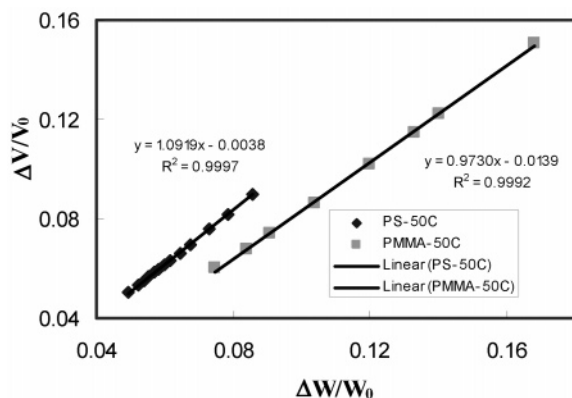


Figure 7. Plot of $\Delta V/V_0$ (volume increases upon swelling/volume of the dry film) vs $\Delta W/W_0$ of CO₂ (based on the data of refs 12 and 14).

γ represents the additional fractional free volume imparted by the diluents

$$\gamma(T) = \frac{v_1\gamma_1(T) + v_2\gamma_2(T)}{v_1 + v_2} \quad (7)$$

As usually expressed, v_i is a volume fraction, but there would be only slight modifications in these expressions using weight fraction instead. Ferguson and von Meerwall also consider a variation of the Vrentas and Duda theory that has a form similar to the above. The main physical idea is that the new free volume is shared by

Table 3. The Activation Energy of Pyrene Diffusion in CO₂-Swollen PMMA^a

$\Delta W/W_0$ ^b	0.10	0.11	0.12	0.13	0.14	0.15
E_a /kcal	13.5	13.1	12.5	11.6	10.5	9.2

^a Based on the plot of $\langle \log D \rangle$ vs $1/T$ at 35, 50, and 65 °C. ^b Weight fraction of CO₂ in the equilibrated film.

all diffusing species such that the diffusion constants for all species are related by

$$\frac{1}{B_{d1}} \ln(D(T,v)_1/D(T,0)_1) = \frac{1}{B_{d2}} \ln(D(T,v)_2/D(T,0)_2) \quad (8)$$

The ratio B_{d1}/B_{d2} can also be interpreted as a ratio of the “jumping unit size” required for the two diluents.¹⁷ Thus, in principle, the diffusion constant of our pyrene probe can be related to the self-diffusion of CO₂ in PS and PMMA. Because our pyrene is present in such low concentrations, we may assume that all swelling expressed in the above equations arises from the CO₂ alone and the results displayed in Figure 6 are consistent with the idea that s_{PS} is substantially larger than s_{PMMA} .

The other striking thing about the data presented in Figure 6 is the relatively strong temperature dependence of $\langle \log D \rangle_{PMMA}$ compared to $\langle \log D \rangle_{PS}$ (note that the correction according to temperature, $D = kT/\zeta$, where ζ is the friction factor, is very small, i.e., comparing 35 and 65 °C $\log(308/338) = -.040$). Evidently, in PMMA, there is a significant “activation energy” associated with pyrene diffusion, although the present data do not elucidate the physical nature of this thermally activated process (e.g., is the activation energy related to the dynamics of the creation or loss of free volume that permits pyrene movement or a local friction factor that depends on more than just the gross amount of free volume). The diffusion activation energy of pyrene in PMMA has been estimated from the plot of $\langle \log D \rangle$ vs $1/T$ at 35, 50, and 65 °C to be around 12 kcal/mol for a CO₂ weight fraction between 0.10 and 0.15 (see Table 3). Obviously, with only three temperature points, these values are not very accurate.

Summary

In the present experiments, we have measured the effect of CO₂ swelling on the transport of a fluorescent probe molecule (pyrene) out of PMMA films. As expected, CO₂ swelling enhances these diffusion constants by orders of magnitude and the relative enhancement is the greatest at the lowest temperature studied (35 °C) because of the higher solubility of CO₂. In comparing

these results with our earlier results for PS films, we find at a given pressure of CO₂ that the enhancement in PMMA is larger, but this just reflects the higher solubility of CO₂ in PMMA compared to PS. When the diffusion constants are compared as a function of weight fraction of CO₂, we find that the diffusion constant in PS exceeds that in PMMA by as much as 4 orders of magnitude. This effect is ascribed to the larger amount of free volume liberated in PS by CO₂ swelling compared to PMMA, although we cannot discount specific "chemical effects" that allow CO₂ to reduce the interaction between pyrene and PS to a greater extent than for PMMA. We also note that the pyrene diffusion constant in PMMA exhibits considerably more temperature dependence than for PS, implying some activation barrier that must be overcome in PMMA in order to effect pyrene diffusion.

Acknowledgment. This work has been supported by the STC Program of the National Science Foundation under Agreement No. CHE-9876674, the Welch Foundation (K.P.J. F-1319 and S.E.W. F-356), and the Separations Research Program at the University of Texas. The DSC experiments were carried out in the Texas Materials Institute Polymer Characterization Laboratory, and we would like to thank Prof. C. G. Willson for allowing us to use his profilometer. We would like to thank Griffin Smith for the help in CO₂ fugacity calculation.

Supporting Information Available: PMMA and PS data. This material is available free of charge via the Internet at <http://pubs.acs.org>.

References and Notes

- (1) (a) Alessi, P.; Cortes, A.; Kikic, I.; Vocchine, F. *J. Appl. Polym. Sci.* **2003**, *88*, 2189–93. (b) Hachisuka, H.; Sato, T.; Imai, T.; Tsujita, Y.; Takizawa, A.; Kinoshita, T. *Polym. J. (Tokyo)* **1990**, *22*, 77–79. (c) Condo, P. D.; Paul, D. R.; Johnston, K. P. *Macromolecules* **1994**, *27*, 365–71. (d) Wang, W.; Chou, V.; Kramer, E. J.; Sachse, W. H. *J. Polym. Sci., Part B: Polym. Phys.* **1982**, *20*, 1371–84.
- (2) Berens, A. R.; Huvar, G. S.; Korsmeyer, R. W.; Junig, F. W. *J. Appl. Polym. Sci.* **1992**, *46*, 231.
- (3) (a) Lu, X.; Manners, I.; Winnik, M. A. In *New Trends in Fluorescence Spectroscopy: Applications to Chemical and Life Sciences*; Valeur, B., Brochon, J.-C., Eds.; Springer: New York, 2001, pp 229–55. (b) Rharbi, Y.; Winnik, M. A. *Adv. Colloid Interface Sci.* **2001**, *89–90*, 25–46 and references therein.
- (4) (a) Ellison, C. J.; Torkelson, J. M. *Nat. Mater.* **2003**, *2*, 695–700. (b) Hall, D. B.; Hamilton, K. E.; Miller, R. D.; Torkelson, J. M. *Macromolecules* **1999**, *32*, 8052–58. (c) Hall, D. B.; Torkelson, J. M.; *Macromolecules* **1998**, *31*, 8817–25. (d) O'Neil, G. A.; Torkelson, J. M. *Macromolecules* **1997**, *30*, 5560–62.
- (5) Gupta, R. R.; RamachandraRao, V. S.; Watkins, J. J. *Macromolecules* **2003**, *36*, 1295–303.
- (6) Cao, T.; Johnston, K. P.; Webber, S. E. *Macromolecules* **2004**, *37*, 1897–902.
- (7) (a) Johnston, K. P.; Eckert, C. A. *AIChE J.* **1981**, *27*, 73–779. (b) Johnston, K. P.; Ziger, D. H.; Eckert, C. A. *Ind. Eng. Chem. Fundam.* **1982**, *21*, 191–7.
- (8) Verification that the release time scales as l^2 was done to ensure that we are dealing with Fickian diffusion.
- (9) Ellison, C. J.; Torkelson, J. M. *J. Polym. Sci., Part B: Polym. Phys.* **2002**, *40*, 2745–58. See Figure 4.
- (10) (a) Crank, J. *The Mathematics of Diffusion*, 2nd ed.; Clarendon Press: Oxford, 1975; Chapter 4. (b) Crank, J.; Park, G. S. *Diffusion in Polymers*; Academic Press: London and New York, Chapter 1, 1968.
- (11) Wissinger, R. G.; Paulaitis, M. E. *J. Polym. Sci., Part B: Polym. Phys.* **1987**, *25*, 2507–10. The relationship between wt% of CO₂ in PS films and pressure were obtained by extrapolating their data.
- (12) Zhang, Y.; Gangwani, K. K.; Lemert, R. M. *J. Supercrit. Fluids* **1997**, *11*, 115–34.
- (13) Hilic, S.; Boyer, S. A.; Padua, A. A. H.; Grolier, J.-P. E. *J. Polym. Sci., Part B: Polym. Phys.* **2001**, *39*, 2063–70.
- (14) Ely, J. F. CO2PAC: A Computer Program to Calculate Physical Properties of Pure CO₂; National Institute of Standards and Technology: Washington, DC, 1986.
- (15) Anwand, D.; Müller, F. W.; Strehmel, B.; Schiller, F. *Makromol. Chem.* **1991**, *192*, 1981–91.
- (16) Ferguson, R. D.; von Meerwall, E. *J. Polym. Sci., Part B: Polym. Phys.* **1980**, *18*, 1285–1301.
- (17) Wisnudel, M. B.; Torkelson, J. M. *Macromolecules* **1996**, *29*, 6193–207.

MA047953S